International Journal of Application or Innovation in Engineering & Management (IJAIEM)
Web Site: www.ijaiem.org Email: editor@ijaiem.org
Volume 6, Issue 5, May 2017 **ISSN 2319 - 4847**

A Comparison of Hyper spectral and Multispectral Datasets for Crop Type Mapping

Maheswarappa B[1], Dr.H.R.Sudarshan Reddy[2]

[1]Dept. of Electronics and Communication, S T J I T, Ranebennur

[2]Professor, Dept. of Electrical & Electronics Engineering., University B.D.T.College of Engineering, Davangere.

Abstract

Atmospheric correction is the one of the major part of a satellite image processing, FLAASH (Fast-Line-of-Sight Atmospheric Analysis of the Spectral Hyper cubes) is efficient method for atmospheric correction of Hyper spectral data. Same spatial resolution, same methodology, different classification results due to different spectral resolution. Mixing of classes is rare in Hyper spectral data as compared to Multi spectral data.

Key words: FLAASH, Hyper spectral data, Multi spectral data and Spatial resolution.

Introduction

Multispectral imagery is produced by sensors that measure reflected energy within several specific sections (also called bands) of the electromagnetic spectrum. Multispectral sensors usually have between 3 and 10 different band measurements in each pixel of the images they produce[1],[2]. Examples of bands in these sensors typically include visible green, visible red, near infrared, etc. Landsat, Quickbird, and Spot satellites are well-known satellite sensors that use multispectral sensors. Hyperspectral sensors measure energy in narrower and more numerous bands than multispectral sensors[3],[2]. Hyperspectral images can contain as many as 200 (or more) contiguous spectral bands. The numerous narrow bands of hyperspectral sensors provide a continuous spectral measurement across the entire electromagnetic spectrum and therefore are more sensitive to subtle variations in reflected energy. Images produced from hyperspectral sensors contain much more data than images from multispectral sensors and have a greater potential to detect differences among land and water features[6],[7].

For example, multispectral imagery can be used to map forested areas, while hyperspectral imagery can be used to map diseases within the crop.

Study Area

Davanagere District and its near by area is selected for this study. In the month of September, Rice is the major crop in that area. Additionally areca nut, some orchard trees also located in that area.

Satellite Datasets

Specification of images used in this study are;

Table 1: Image specification of Hyperion data

Sl. No	Location	Acquisition date	Spectral Resolution	Spatial Resolution
1	Latitude :14.4663 Longitude: 75.9238	22 Sep, 2015	242	30m

Table 2: Image specification of Landsat ETM+ data

S. No.	Location	Acquisition date	Spectral Resolution	Spatial Resolution
1	Latitude :14.4663 Longitude: 75.9238	06 Sep 2015	7	30m (Band 1-5,7) 60 m (Band 6)

Methodology

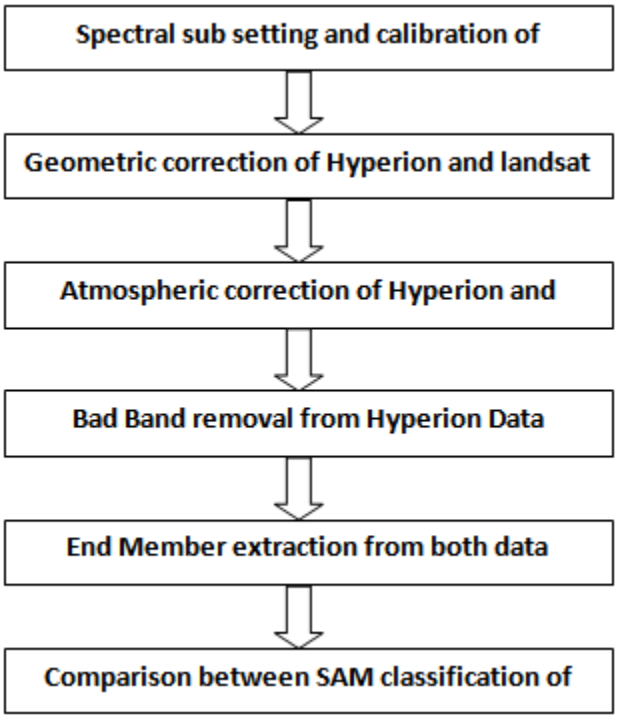

Spectral sub-setting and calibration of Hyperion image

Out of 242 bands, Hyperion acquire data in 196 bands. Because of this reason spectral sub-setting was done in the first step. For radiometric calibration VNIR bands were divided by 40 where as SWIR bands were divided by 80 as directed in user manual of Hyperion data sets. Hyperion data was geometrically corrected using ENVI image registration tool and Land sat ETM image was used as referenced image. A cell size used is 30 meters and WGS-84 Datum , Nearest Neighbor method is used for the resampling.

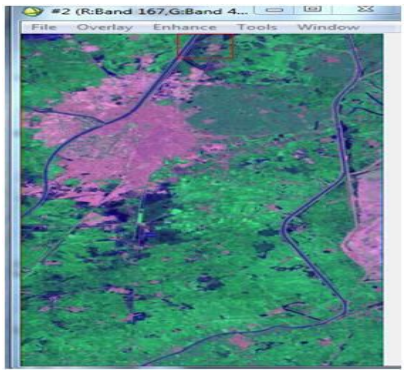

Fig 1: Multispectral image

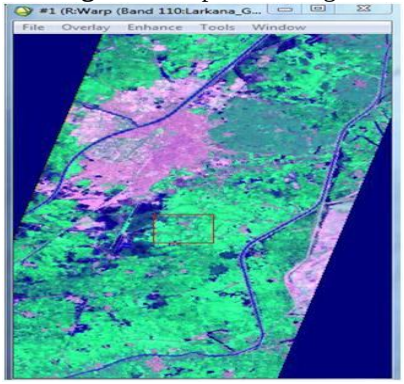

Fig 2: Hyperspectral image

Atmospheric Correction Using FLAASH

Atmospheric correction of the 196 channels of Hyperion data set was performed by using FLAASH (Fast Line-of-Sight Atmospheric Analysis of the Spectral Hyper cubes).

The use of reflectance instead of radiances results into two advantages.

1. First, the cosine effect of different solar zenith angles due to the time difference between data acquisition scan bere moved.
2. Second, it compensates for different values of the exoatmospheric solar irradiances arising from spectral band differences.

$$\rho_p = \left(\pi \times L_\lambda \times D^2\right) / \left(E_{SUN\lambda} \times \cos\left(\theta_{zenith}\right)\right) \quad (1)$$

Where,

ρ_p: Unit less planetary reflectance
L_λ: Spectral radiance at the sensor's aperture
D: Earth-Sun distance in astronomical units
$E_{SUN\lambda}$: Mean solar exoatmospheric irradiances
θ_{zenith}: Solar zenith angle in degrees

Radiometric Correction: To remove disturbances by the atmosphere digital numbers (DN)are converted to at-satellite radiance based on the gain (L_{max}) and bias (L_{min}) for each band (MarkhamandBarker,1986), which were provided from image header file.

$L_{\lambda sensor} = ((L_{max} - L_{min}) / Q_{calmax}) * Q_{cal} + L_{min}$ (2)

Where,

$L_{\lambda sensor}$: Spectral Radiance at the sensor's aperture In W/(m2.sr. μm)
Q_{cal}: The quantized calibrated pixel value in Digital Number (DN)
Q_{calmax}: The maximum quantized calibrated pixel value (DN=255) corresponding to Lmax
L_{min}: The spectral radiance that is scaled to Qcalminin W/(m2.sr. μm)
L_{max}: The spectral radiance that is scaled to Qcalmaxin W/(m2.sr. μm)

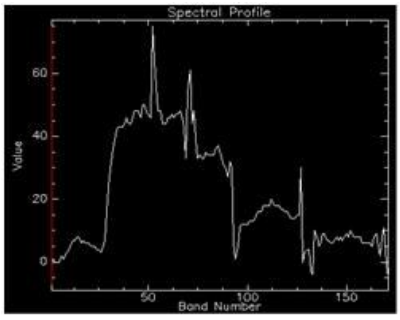

Fig 3: Before Correction

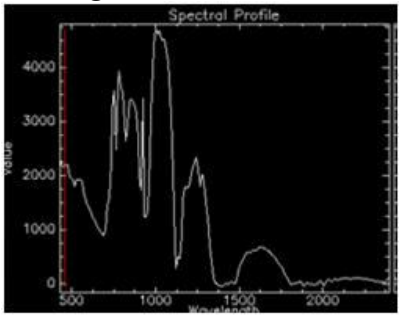

Fig 4: After Correction

Bad Band Selection: Atmospheric water vapor bands have vertical stripping that are usually identified by visual (Beck R et. al.,2003). For this reason, the sub set of 129 selected bands incorporated for SAM classification are listed in below table.

Table 3: List of selected 129 bands used for this research

Array	Bands	Wavelengths (nm)
VNIR	5-46	467.52 –884.7
	55-68	972.99 –1104.12
SVIR	74-90	1164.68 –1326.05
	107-135	1164.68 –1326.05
	154-156	1971.76 –1991.96
	160-171	2032.35 –2143.34
	176-190	2193.73 –2335.01

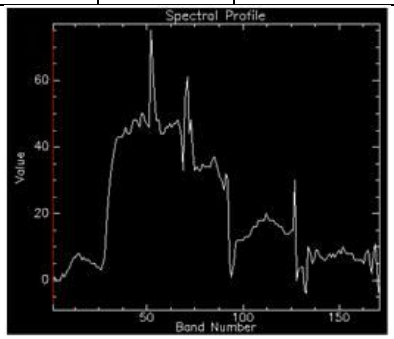

Fig 5: Before Correction

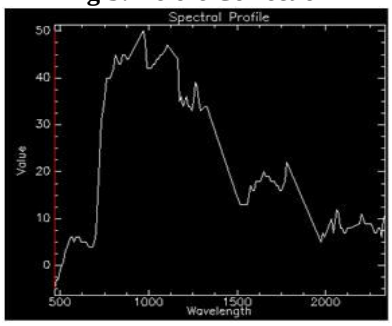

Fig 6: After correction

End – Member Extraction: Theoretically the existing pure features in mixed pixels are referred to a send-members. Field based spectral libraries for end-member extraction were unavailable. Image based spectral libraries were used for SAM classification. A window of 3x3 pixels was used for the extraction of spectral end-members of each feature.

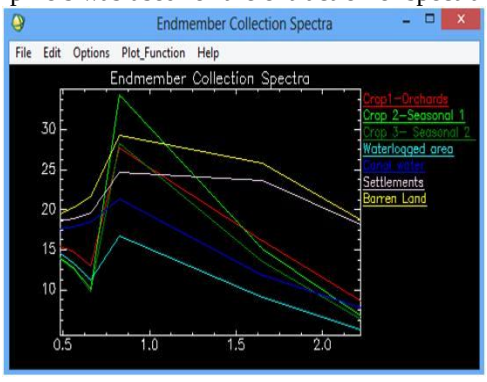

Fig 7: Multispectral Data

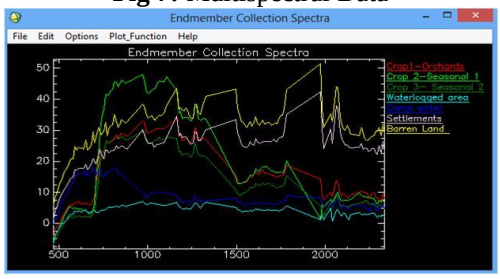

Fig 8: Hyperspectral Data

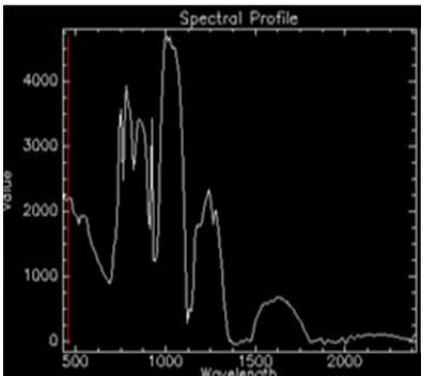

Fig 9: Multispectral Data

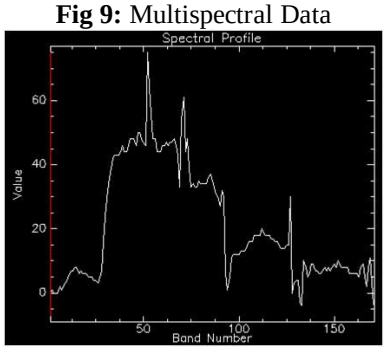

Fig 10: Hyperspectral Data

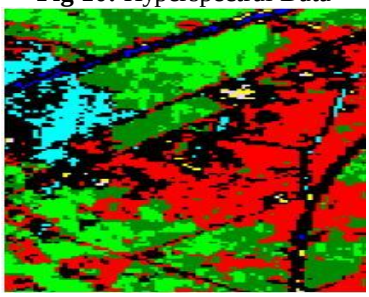

Fig 11: Multispectral Data

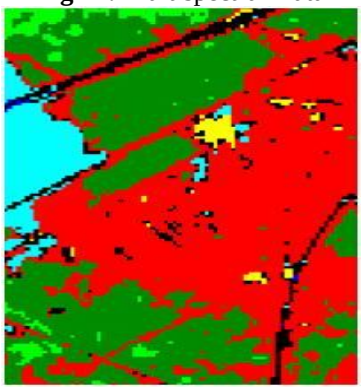

Fig 12: Hyperspectral Data

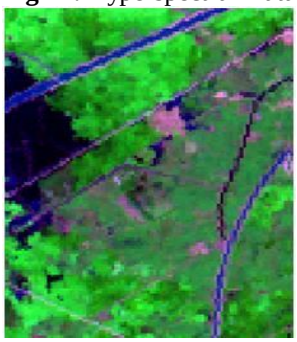

Fig 14: Unclassified Image

Spectral Angular Mapper Classification: In this study, the Spectral Angle Mapper (SAM) classification is applied for crop type mapping. The Spectral Angle Mapper (SAM) is a physically – based spectral classification that uses an n-dimensional angle to match pixels to reference spectra [Kruse *et al.*,1993].

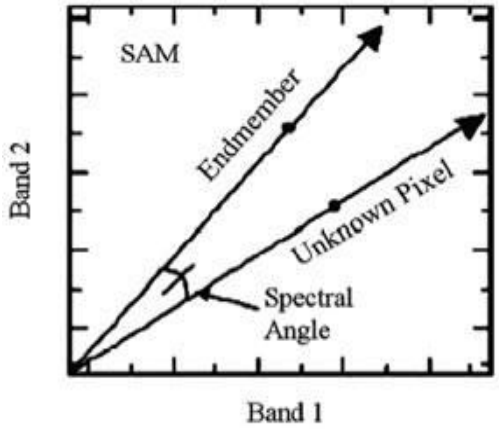

Fig 15: SAM response

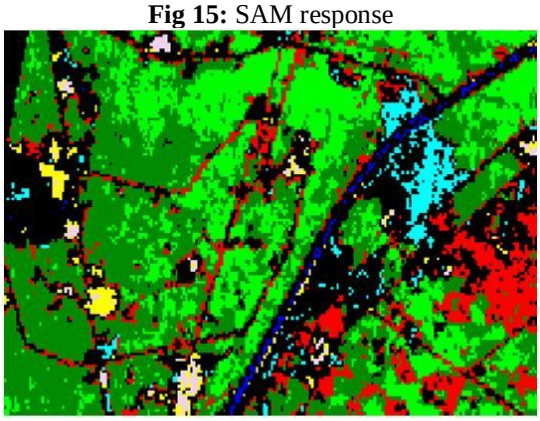

Fig 16: Multispectral Image

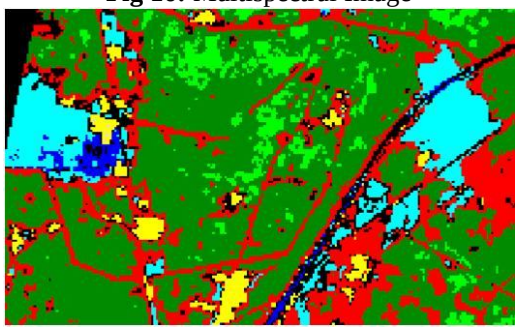

Fig 17: Hyperspectral Image

Conclusion

It is concluded that FLAASH(Fast Line-of- Sight Atmospheric Analysis of the Spectral Hyper cubes) is efficient method for atmospheric correction of Hyper spectral data, we observe that Same spatial resolution, same methodology, different classification results due to different spectral resolution and Mixing of classes is rare in Hyperspectral data as compared to Multispectral data. Finally we concluded that due to high resolution hyperspectral data yields the efficient classification compare to the multispectral data .

References

[1] Thenkabail, Prasad S., et al. Selection of Hyperspectral Narrowbands (HNBs) and Composition of Hyperspectral Two Band Vegetation Indices (HVIs) for Biophysical Characterization and Discrimination of Crop Types Using Field Reflectance and Hyperion/EO-1 Data. Selected Topics in Applied Earth Observations and Remote Sensing, IEEE Journal of 6.2. 2013. 427-439.

[2] Shwetank, S., Kamal Jain, and Karamjit Bhatia. Development of Digital Spectral Library and Supervised Classification of Rice Crop Varieties Using Hyperspectral Image Processing. Asian Journal of Geoinformatics. 2012. 11.3.
[3] H. North, D. Painnan, S. E. Belliss and J. Cuff, "Classitying Agricultural Land Uses with Time Series of Satellite Images," Int. Geosci. Remote Sens. Symp. (IGARSS '20J2), pp.5693-5696. 20 12.
[4] B.Wu and Q. Li, "Crop planting and type proportion method for crop acreage estimation of complex agricultural landscapes," Int. J. Appl. Earth Obs. Geoinform. 16, 101–112 (2012),
[5] Roberts, Dar A., Keely L. Roth, and Ryan L. Perroy. Hyperspectral Vegetation Indices. Hyperspectral Remote Sensing of Vegetation. 2011. 309.
[6] C. Boryan, Z. Yang, R. Mueller, and M. Craig, "Monitoring US agriculture: The US Department of Agriculture, National Agricultural Statistics Service, Cropland Data Layer Program," Geocarto Int., vol. 26, no. 5, pp. 341–358, 2011.
[7] K. Jia et al., "Vegetation classification method with biochemical composition estimated from remote sensing data," Int. J. Remote Sens. 32(24), 9307–9325 (2011),
[8] J. de Leeuw, Y. Georgiadou, N. erle, A. de Gier, Y. Inoue, J. Ferwerda, M. Smies, and D. Narantuya, "The function of remote sensing in support of environmental policy," Remote Sens., vol. 2, no. 7, pp. 1731–1750, Jul. 2010.
[9] M. Ozdogan, "The Spatial Distribution of Crop Types from MODIS Data: Temporal Unmixing Using Independent Components Analysis," Remote Sens. Env. , vol. 1 1 4, pp. 1 1 90- 1 204, 20 1 0 .
[10] Wan, Zhengming, and Z.-L. Li, 1997, "A Physics-Based Algorithm for Retrieving Land-Surface Emissivity and Temperature from EOS/MODIS Data," IEEE Transactions on Geoscience and Remote Sensing, Vol. 35, pp. 980-996.